γ-Tubulin–like Tub4p of *Saccharomyces cerevisiae* Is Associated with the Spindle Pole Body Substructures That Organize Microtubules and Is Required for Mitotic Spindle Formation

Anne Spang, Silke Geissler, Katrin Grein, and Elmar Schiebel

Max-Planck-Institut für Biochemie, Genzentrum, D-82152 Martinsried, Germany

Abstract. Tub4p is a novel tubulin in *Saccharomyces cerevisiae* that most closely resembles γ-tubulin. We report in this manuscript that the essential Tub4p is associated with the inner and outer plaques of the yeast microtubule organizing center, the spindle pole body (SPB). These SPB substructures are involved in the attachment of the nuclear and cytoplasmic microtubules, respectively (Byers, B., and L. Goetsch. 1975. *J. Bacteriol.* 124:511–523). Study of a temperature sensitive *tub4-1* allele revealed that *TUB4* has essential functions in microtubule organization. Remarkably, SPB duplication and separation are not impaired in *tub4-1* cells incubated at the nonpermissive temperature. However, SPBs from such cells contain less or misdirected nuclear microtubules. Further analysis revealed that *tub4-1* cells are able to assemble a short bipolar spindle, suggesting that the defect in microtubule organization occurs after spindle formation. A role of Tub4p in microtubule organization is further suggested by an increase in chromosome loss in *tub4-1* cells. In addition, cell cycle arrest and survival of *tub4-1* cells is dependent on the mitotic checkpoint control gene *BUB2* (Hoyt, M.A., L. Totis, B.T. Roberts. 1991. *Cell.* 66:507–517), one of the cell's monitors of spindle integrity.

THE number, direction, and polarity of microtubules are organized by organelles called microtubule organizing centers (MTOC)[1]. In *Saccharomyces cerevisiae*, microtubule organizing functions are provided by the spindle pole body (SPB) (see Fig. 8 *A*). The SPB is a cylindrical multilaminated structure that is embedded in the nuclear envelope. SPB substructures are detectable by EM (Byers, 1981*a*,*b*; Byers and Goetsch, 1975). The central plaque serves to anchor the SPB in the nuclear envelope. The inner and outer plaques nucleate the nuclear and cytoplasmic microtubules, respectively. An additional substructure of the SPB, the half bridge, is an extension of the central plaque along the cytoplasmic margin of the nuclear envelope. The half bridge has important functions in SPB duplication.

The SPB, in common with centrosomes of higher eukaryotes, shows cell cycle–dependent behavior (Byers and Goetsch, 1975). In G1 of the cell cycle, the single SPB in each yeast cell is duplicated. The duplicated SPBs undergo separation to form the poles of the spindle. Motor proteins and microtubules are required for SPB separation and spindle formation (Jacobs et al., 1988; Saunders and Hoyt, 1992). In mitosis, nuclear microtubules organized by the inner plaque of the SPB have essential functions in chromosome segregation (Jacobs et al., 1988). Cytoplasmic microtubules are required for the migration of the nucleus into the bud, but they are not essential for spindle elongation in anaphase B (Sullivan and Huffaker, 1992). Interestingly, a surveillance system involving the *BUB* (Hoyt et al., 1991) and *MAD* genes (Li and Murray, 1991) halts the cell cycle in mitosis in response to microtubule perturbation. After nuclear division and cytokinesis, each yeast cell retains exactly one SPB.

MTOCs from phylogenetically different organisms are heterogeneous in structure. Despite these structural differences, MTOCs contain related proteins that may perform similar functions. Phylogenetically conserved components of MTOCs are centrin (Baum et al., 1986; Errabolu et al., 1994; Lee and Huang, 1993; Salisbury et al., 1984; Spang et al., 1993) and γ-tubulin (Horio et al., 1991; Oakley et al., 1990; Stearns et al., 1991; Zheng et al., 1991). γ-Tubulin is, besides α- and β-tubulin, the third member of the tubulin superfamily. It is assumed that γ-tubulin is a key component of MTOCs involved in microtubule nucleation (Joshi et al., 1992; Stearns and Kirschner, 1994). This conclusion is consistent with the inhibition of microtubule nucleation after disruption of the essential γ-tubulin genes in *Aspergillus nidulans* (Oakley et al., 1990), *Schizosaccharomyces pombe* (Horio et al., 1991), and *Drosophila* (Sunkel et al., 1995), and by the failure of mammalian cells to assemble mitotic spindles after microinjection of anti–γ-tubulin antibodies (Joshi et al., 1992). Furthermore, γ-tubulin binds in

Address all correspondence to Elmar Schiebel, Max-Planck-Institut für Biochemie, Genzentrum, Am Klopferspitz 18a, D-82152 Martinsried, Germany. Tel.: (49) 89-85-78-38-10. Fax: (49) 89-85-78-38-10.

1. *Abbreviations used in this paper:* ADH, alcohol dehydrogenase; DAPI, 4′,6-diamidino-2-phenylindole; 5-FOA, 5-fluroorotic acid; GST, glutathione-*S*-transferase; HA, hemagglutinin; HU, hydroxyurea; MTOC, microtubule organizing center; SC, synthetic complete medium; SPB, spindle pole body; YPD, yeast extract, peptone, and dextrose growth medium.

vitro with high affinity to the minus end of microtubules (Li and Joshi, 1995) that are proximal to the MTOC (McIntosh and Euteneuer, 1984). A highly purified γ-tubulin complex from *Xenopus* consists of at least seven different proteins and seems to have an open ring structure. This complex caps the minus end of microtubules in vitro (Zheng et al., 1995) and in situ (Moritz et al., 1995).

Besides α- and β-tubulin, a novel tubulin, Tub4p, that most resembles γ-tubulin has been identified by the yeast genome sequencing project in *S. cerevisiae.* Due to the relatively low identity to any of the three tubulin subfamilies, it has been suggested that Tub4p represents a new class of tubulin (Burns, 1995). While our manuscript was in preparation, Sobel and Snyder (1995) reported that an epitope-tagged Tub4p resides at the SPB. Partial depletion of Tub4p caused a nuclear migration failure and multiple defects in spindle formation after 17–20 h. Since Tub4p levels were not controlled in these experiments, it remains unclear whether the observed defects are a direct or indirect consequence of Tub4p depletion.

In this paper we confirm the association of Tub4p with the SPB and report that the essential Tub4p is associated with the inner and outer plaques of the SPB. These SPB substructures are involved in the organization of the nuclear and cytoplasmic microtubules, respectively. A function of Tub4p in microtubule organization is suggested by the phenotype of the conditional lethal *tub4-1* allele, which arrests in the first cell cycle after shifting the cells to the nonpermissive temperature. SPB duplication, SPB separation, and spindle formation were normal in *tub4-1* cells. However, no mitotic spindles were observed. In addition, defects in microtubule organization of *tub4-1* cells are indicated by an increase in chromosome loss and by the dependence of cell cycle arrest and survival on the mitotic checkpoint control gene *BUB2*, which is involved in monitoring spindle integrity.

Materials and Methods

Yeast Strains, Media, and Yeast Transformation

Yeast strains used in this study are summarized in Table I. Yeast cells were grown in yeast extract, peptone, and dextrose growth medium (YPD). Synthetic complete medium (SC) was prepared as described by Guthrie and Fink (1991) with glucose, raffinose, or galactose as carbon sources. Yeast strains were transformed as described by Schiestl and Gietz (1989).

DNA Techniques

PCR was performed with Vent polymerase supplied by New England Biolabs (Beverly, MA). The nucleotide sequence of all PCR products was confirmed by the chain-termination method of Sanger et al. (1977) using synthetic primers. DNA fragments were purified with the Geneclean II kit from Bio 101, Inc. (Vista, CA) according to the manufacturer's recommendation. DNA manipulations were performed as described by Sambrook et al. (1989).

Cloning of TUB4 by PCR

The entire *TUB4* was amplified by PCR with primers TUB4-1 (5′-CAACTCTAGATAGTCACAGCAATAATGTC-3′) and TUB4-2 (5′-CCAATGCATCCTGTTCGGCGTCCTC-3′) using chromosomal DNA from strain S288C as template (These sequence data are available from EMBL/GenBank/DDBJ under accession number YSCH8167). Primers TUB4-1 and TUB4-2 carry an XbaI and NsiI restriction site, respectively. The 2,200-bp PCR product was restricted with XbaI and NsiI and ligated into pRS315 (Sikorski and Hieter, 1989), previously restricted with XbaI and PstI to give plasmid pSM204. *TUB4* on pRS316 was named pSM223.

Plasmid Constructions

Construction of a GST–Δtub4 Gene Fusion. The 600-bp EcoRI/SalI fragment of pSM204 carrying the 3′ end of *TUB4* was cloned into the EcoRI/XhoI sites of the glutathione-*S*-transferase (GST) expression vector pGEX-5X-1 (Pharmacia, Uppsala, Sweden). The resulting plasmid was named pSM220.

Construction of Epitope-tagged TUB4–HA Gene Fusions. An NotI restriction site was introduced by PCR between the coding region of *TUB4* and the TAA stop codon using primers TUB4-4 (5′-TCATTAGCGGCCGCTTACTAATTTATGATCACCGTCG-3′) and TUB4-5 (5′-TTAGTAAGCGGCCGCTAATGATGCCTTCCTTGTTCAGG-3′). The resulting plasmid was named pSM217. The 114-bp NotI fragment of plasmid pGTEP-I (kindly provided by B. Futcher, Cold Spring Harbor, NY) with three repeats coding for the hemagglutinin epitope (YPYDVPDYA) was inserted into the NotI restriction site of pSM217. The orientation and number of inserts were confirmed by sequencing. Plasmid pSM218 carries a single insertion of the 114-bp NotI-fragment (*TUB4-HA* gene fusion).

TUB4 under the Control of the GAL1 Promoter. The coding region of *TUB4* was amplified by PCR with primers TUB4-3 (5′-CGGGGTACCATGGGTGGAGAAATTATTA C-3′) and TUB4-2. Primer TUB4-3 introduces a KpnI restriction site upstream of the start codon of *TUB4.* The PCR product was restricted with KpnI and NsiI and cloned into the KpnI and PstI sites of vector pQE30 (Qiagen, Inc., Chatsworth, CA) to give plasmid pSM205. Plasmid pSM205 was restricted with KpnI and SalI. The SalI restriction site is located in the polylinker region of pQE30 next to the PstI site. The KpnI/SalI fragment of pSM205 with the coding region of *TUB4* was cloned into the yeast expression vector pYES2 (Invitrogen, San Diego, CA), which was restricted with KpnI and XhoI. The resulting plasmid pSM209 carries a *GAL1–TUB4* fusion.

Expression of γ-tubulin from Xenopus in Yeast. The alcohol dehydrogenase (ADH) promoter/terminator from pHD605 (kindly provided by H. Domdey, Genzentrum, Munich, Germany) was cloned into plasmid pBlue SK (Stratagene, La Jolla, CA) to give pBlue-ADH. γ-tubulin from *Xenopus laevis* on plasmid pTS235 (kindly provided by T. Stearns, Stanford University, CA) (Stearns et al., 1991) was amplified by PCR with primers JIC-III (5′-CAGCTGATGCATTTATTTATCCTGGGTTCCCCACG-3′) and JIC-IV (5′-AGATTTGAATTCATGCCACGGGAGATTATCAC-3′). The PCR product was treated with the Sure clone kit (Pharmacia), and then cloned into the HindIII restriction site of pBlue-ADH that had been converted to blunt end with Klenow polymerase (pSS1-2). The ADH–γ-tubulin fusion on a 3,500-bp XhoI/PvuII fragment was cloned into *LEU2*-based vector pRS315 (Sikorski and Hieter, 1989). The resulting plasmid was named pSM83.

Construction of a Δtub4::HIS3 Disruption Cassette. *TUB4* of pSM204 was restricted with Eco47III and PstI, disrupting the coding region of *TUB4. HIS3* on a SmaI/NsiI fragment was inserted into *TUB4* (pSM208). The Δtub4::HIS3 on an SacI/SalI fragment from pSM208 was ligated into vector pBlue SK that was restricted with SacI and SalI (pSM219).

Construction of a bub2::HIS3 Disruption Cassette. *BUB2* was cloned by PCR using chromosomal DNA from strain S288C (gift of R. Mortimer, University of California, Berkeley). The PCR product was subcloned into pUC18 using the Sure clone kit from Pharmacia (pSM51). *HIS3* on an SmaI fragment was ligated with pSM51 previously restricted with EcoRV (pSM63). The EcoRV site is located just downstream of the *BUB2* start codon.

Construction of tub4-1(ts)

TUB4 was mutagenized by PCR according to Cadwell and Joyce (1992). The PCR product was restricted with XbaI and NsiI, and then cloned into the XbaI and PstI sites of plasmid pRS315 (Sikorski and Hieter, 1989). A pool of plasmids were transformed into strain ESM183, and selection was made on SC plates lacking uracil and leucine. Cells, which had lost pSM223, were selected by growth on 5-fluoroorotic acid (5-FOA) plates at 23°C. The Ura$^-$ colonies were tested for growth at 23° and 37°C. DNA from strains, which could not grow at 37°C, was isolated and transformed into *Escherichia coli* Sure. Plasmid-DNA was then again transformed into ESM183. Transformants were incubated on 5-FOA plates at 23°C, and then tested for temperature sensitivity on YPD plates. The nucleotide sequence of *tub4(ts)* alleles was analyzed.

Table I. Yeast Strains

Strain	Genotype	Source or reference
S288C	*MATα mal gal2*	R. Mortimer (University of California, Berkeley)
BJ5626	*MATa/α ura3-52/ura3-52 trp1/TRP1 leu2Δ1/LEU2 his3Δ200/his3Δ200 pep4::HIS3/pep4::HIS3 prb1Δ1.6R/prb1Δ1.6R can1/can1*	B. Jones (Carnegie-Mellon University, Pittsburgh, PA)
YPH499	*MATa ura3-52 lys2-801 ade2-101 trp1Δ63 his3Δ200 leu2Δ1*	Sikorski and Hieter (1989)
YPH500	*MATα ura3-52 lys2-801 ade2-101 trp1Δ63 his3Δ200 leu2Δ1*	Sikorski and Hieter (1989)
YPH501	*MATa/α ura3-52/ura3-52 lys2-801/lys2-801 ade2-101/ade2-101 trp1Δ63/trp1Δ63 his3Δ200/his3Δ200 leu2Δ1/leu2Δ1*	Sikorski and Hieter (1989)
ESM176	*MATa ura3-52 lys2-801 ade2-101 trp1Δ63 his3Δ200 leu2Δ1* pYES2	this study
ESM177	*MATa ura3-52 lys2-801 ade2-101 trp1Δ63 his3Δ200 leu2Δ1* pSM209§	this study
ESM178	*MATa/α ura3-52/ura3-52 lys2-801/lys2-801 ade2-101/ade2-101 trp1Δ63/trp1Δ63 his3Δ200/his3Δ200 leu2Δ1/leu2Δ1 TUB4/Δtub4::HIS3*	this study
ESM183	*MATa ura3-52 lys2-801 ade2-101 trp1Δ63 his3Δ200 leu2Δ1 Δtub4::HIS3* pSM223*	this study
ESM184	*MATa ura3-52 lys2-801 ade2-101 trp1Δ63 his3Δ200 leu2Δ1 Δtub4::HIS3* pSM222‡	this study
ESM204	*MATα ura3-52 lys2-801 ade2-101 trp1Δ63 his3Δ200 leu2Δ1 ΔTUB4*::pSM244‖	this study
ESM208	*MATα ura3-52 lys2-801 ade2-101 trp1Δ63 his3Δ200 leu2Δ1 tub4-1*	this study
ESM210	*MATa/α ura3-52/ura3-52 lys2-801/lys2-801 ade2-101/ade2-101 trp1Δ63/trp1Δ63 his3Δ200/his3Δ200 leu2Δ1/leu2Δ1 TUB4/tub4-1*	this study
ESM215	*MATα ura3-52 lys2-801 ade2-101 trp1Δ63 his3Δ200 leu2Δ1 tub4-1 bub2::HIS3*	this study
ESM218	*MATa ura3-52 lys2-801 ade2-101 trp1Δ63 his3Δ200 leu2Δ1 tub4-1*	this study
YRN212	*MATα ura3-52 lys2-801 ade2-101 trp1Δ1 cyh^{R}2 [CF(CEN6) TRP1 SUP11 CYH^{S}2]*	J. Hegemann (University of Giessen, Germany)
YAS3	*MATα ura3-52 lys2-801 ade2-101 trp1Δ1 cyh^{R}2 [CF(CEN6) TRP1 SUP11 CYH^{S}2] TUB*::pSM244¶	this study
YAS4	*MATα ura3-52 lys2-801 ade2-101 trp1Δ1 cyh^{R}2 [CF(CEN6) TRP1 SUP11 CYH^{S}2] tub4-1*	this study
YAS5	*MATa ura3-52 lys2-801 ade2-101 trp1Δ63 his3Δ200 leu2Δ1 tub4-1 Δsst1::URA3*	this study
YAS7	*MATa ura3-52 lys2-801 ade2-101 trp1Δ63 his3Δ200 leu2Δ1 Δsst1::URA3*	this study
YAS9	*MATa ura3-52 ade2-101 trp1Δ63 leu2Δ1 cdc15 Δsst1::URA3*	this study

*pSM223 is a pRS316 (Sikorski and Hieter, 1989) derivative carrying *TUB4*.
‡pSM222 is a pRS316 derivative carrying *TUB4-HA*.
§pSM209 is a pYES2 derivative containing *GAL-TUB4*.
¶pSM 244 is a pRS306 derivative carrying *tub4-1*.

Construction of Yeast Strains

ESM178. The diploid strain YPH501 (Sikorski and Hieter, 1989) was transformed with the *TUB4* disruption cassette of pSM219 restricted with SalI and SacI, and selection was made on SC plates lacking histidine. The construction of ESM178 was confirmed by Southern analysis as described by Spang et al. (1993).

ESM183. ESM178 was transformed with plasmid pSM223 selection being made on SC plates lacking uracil (ESM181-3). Plasmid pSM223 carries *TUB4* on the *URA3*-based vector pRS316 (Sikorski and Hieter, 1989). ESM181-3 was sporulated and tetrads were dissected. Colonies which were His$^+$ Ura$^+$ were named ESM183. ESM183 carries the *Δtub4::HIS3* disruption and plasmid pSM223.

ESM184. ESM178 was transformed with plasmid pSM222. Transformants were selected on SC plates lacking uracil (ESM181). Plasmid pSM222 carries the *TUB4-HA* of pSM218-4 on pRS316. Spores of ESM181 were obtained (ESM184), which were His$^+$ Ura$^+$, indicating that *TUB4-HA* is functional.

ESM208, YAS3, and YAS4. *tub4-1* was cloned into integration vector pRS306 (Sikorski and Hieter, 1989) to give plasmid pSM244, which was linearized with the restriction enzyme HpaI. Plasmid pSM244 was then integrated into its chromosomal location by homologous recombination, creating a duplication containing the wild-type copy and the mutant copy flanking the plasmid sequences. Strains YPH500 and YRN212 (gift of J. Hegemann, University of Giessen, Germany) were transformed with the linearized plasmid pSM244, with selection being made on SC plates lacking uracil. The transformants were named ESM204 and YAS3, respectively. Integration of plasmid pSM244 was confirmed by Southern analysis. Cells, which spontaneously excised plasmid pRS306 together with *TUB4*, were selected for on 5-FOA plates. Temperature-sensitive colonies derived from ESM204 and YAS3 were named ESM208 and YAS4, respectively.

ESM210, ESM218, YAS5, YAS7, and YAS9. ESM208 was crossed with strain YPH499. The diploid strain ESM210 was sporulated. Two colonies of each tetrad revealed a temperature-sensitive growth defect. One *MATa tub4-1* colony was named ESM218. *SST1* of ESM218, YPH499, and *cdc15* was disrupted with the *Δsst1::URA3* disruption cassette of plasmid pJG-sst-1 (Reneke et al., 1988) to give strains YAS5, YAS7, and YAS9, respectively.

ESM215. *BUB2* of ESM208 was disrupted by the one-step gene replacement method of Rothstein (1983) using the *BUB2::HIS3* disruption cassette of plasmid pSM63.

ESM176 and ESM177. YPH499 was transformed with plasmid pYES2 (ESM176) or pSM209 (ESM177) selection being made on SC lacking uracil.

Affinity-purified Tub4p Antibodies and Anti-Peptide γ-Tubulin Antibodies

GST-ΔTub4p was expressed by the addition of isopropyl β-D-thiogalactoside to the culture medium of *E. coli* Sure (pSM220) as described by Spang et al. (1993). The fusion protein was purified by affinity purification using glutathione Sepharose from Pharmacia. Antibodies against the purified protein were raised in a rabbit as described by Harlow and Lane (1988). The anti-Tub4p antibodies were purified as described by Spang et al. (1995).

Anti-peptide γ-tubulin antibodies (rabbit, polyclonal) were kindly provided by Dr. M. Bornens (Centre National de la Recherche Scientifique, Paris, France). The antibodies were directed against the peptide EEFATEGTDRKDVFFY (amino acids 38–53 of human and *Xenopus* γ-tubulin). The corresponding sequence in Tub4p is PDSSTERDDDDT-KPFFR (identical amino acids are underlined).

Isolation of SPBs, Immunofluorescence, Immunoelectron Microscopy, and Electron Microscopy of Yeast Cells

SPBs were isolated as reported by Rout and Kilmartin (1990). Immunofluorescence and immunoelectron microscopy of yeast cells and SPBs were performed as described by Spang et al. (1995) or by Rout and Kilmartin (1990). All antibodies were from Jackson ImmunoResearch Laboratories (West Grove, PA) unless indicated otherwise. Primary antibodies

were 12CA5 (Hiss Diagnostics GmbH, Freiburg, Germany), anti-90-kD (kindly provided by J. Kilmartin, Medical Research Council, Cambridge, UK) (Rout and Kilmartin, 1990), anti-Karlp (Spang et al., 1995), or affinity-purified anti-Tub4p antibodies. Secondary antibodies in immunofluorescence were rabbit anti-mouse IgG conjugated with FITC and goat anti-rabbit IgG conjugated with CY3.

Immunoelectron microscopy of isolated SPBs was performed as follows: SPBs were embedded into LR White as described by Spang et al. (1993). Sections of enriched SPBs were incubated with mouse monoclonal 12CA5 or anti-β-tubulin (WA3; kindly provided by U. Euteneuer-Schliwa, University of Munich, Germany) antibodies followed by an incubation with rabbit anti-mouse IgGs. Finally, the sections were incubated with protein A bound to gold. Sections of SPBs were also incubated with rabbit anti-Tub4p antibodies. In this case, the second incubation was performed with protein A bound to gold. For double labeling experiments, sections of enriched SPBs were first labeled with mouse monoclonal 12CA5 antibody. After washing, sections were incubated with rabbit anti-mouse IgGs, followed by an incubation with protein A bound to gold. The preparation was fixed with glutaraldehyde for 10 min. The second antibody was either anti-β-tubulin (WA3) or the anti-90-kD antibody. After washing, sections were incubated with goat anti-mouse IgGs coupled to 5 nm gold. No 5-nm signal was observed when the anti-90-kD or anti-tubulin antibodies were omitted from the incubation, indicating that all 12CA5 binding sites were blocked by the rabbit anti-mouse IgGs. Alternatively, the rat monoclonal anti-α-tubulin antibody YOL1/34 (Sera-lab) was used as the second antibody in the double labeling experiment followed by an incubation with rabbit anti-rat IgGs coupled to gold particles. No signal was obtained with secondary antibodies only. Thin-section EM of yeast cells was performed as described by Byers and Goetsch (1991).

Cell Lysates and Immunoblots

Yeast cell lysates were prepared as described by Ausubel et al. (1994). The protein content of samples was measured by the method of Bradford (1976). Proteins were separated by SDS-PAGE (Laemmli, 1970). Immunoblotting was performed as described by Harlow and Lane (1988). Secondary antibodies were goat anti-rabbit or rabbit anti-mouse IgG conjugated with HRP (Bio Rad Laboratories, Hercules, CA). Detection was made by enhanced chemiluminescence using a kit from Amersham Buchler GmbH (Braunschweig, Germany).

Synchronization of Yeast Cells and Flow Cytometry

Cells carrying the *Δsst1::URA3* deletion were incubated with 1 μg/ml synthetic α-factor for 2 h at 23°C. Arrested cells were then incubated for 1 h at 37°C. Cells were released by washing with YPD medium. In some experiments, 0.1 M hydroxyurea (HU) was added to the culture after release from α-factor arrest. The culture was then incubated for 2 h at 37°C. DNA content was determined by flow cytometry as described by Hutter and Eipel (1979).

Overexpression of TUB4 and Immunoblotting

Strains ESM177 (*GAL1-TUB4*) and ESM176 (pYES2) were grown in SC medium lacking uracil with raffinose as a carbon source. Galactose was added to half of the culture at a density of 5×10^6 cells per ml, and glucose was added to the other half. The cultures were incubated for 2–12 h at 30°C. Protein extracts were loaded onto a 10% SDS-PAGE. Immunoblots were incubated with affinity-purified rabbit anti-Tub4p antibodies. To determine overexpression of *TUB4*, the extract of ESM177 was diluted 1:5, 1:25, 1:50, and 1:100. The Tub4p signal obtained in the 1:100 dilution of ESM177 was stronger than that from the undiluted ESM176. Therefore, ESM177 contained at least 100-fold more Tub4p than ESM176.

Sequence Comparison

Protein sequences were compared using the program Bestfit of the GCG package of the University of Wisconsin.

Results

γ-Tubulin from X. laevis Does Not Complement for TUB4

We were interested in whether the γ-tubulin from *X. laevis* (Xgam) expressed in *S. cerevisiae* provides *TUB4* function. Complementation of *TUB4* by *Xgam* would certainly suggest that *TUB4* is the γ-tubulin of *S. cerevisiae.* We constructed strain ESM183 (*Δtub4::HIS3 pSM223*), which has a disruption of *TUB4* and is maintained by *TUB4* on a *URA3*-based plasmid (pSM223). ESM183 did not grow on 5-FOA plates that select against the *URA3*-plasmid, showing that *TUB4* is essential for growth (Fig. 1 *B*, sector 3) (Sobel and Snyder, 1995). In contrast, 5-FOA–resistant colonies were obtained when ESM183 contained an additional *TUB4* on the *LEU2*-based plasmid pSM204 (sector 1). This property of ESM183 was used to test whether *Xgam* expressed from the *ADH* promoter (*ADH-Xgam*) complemented for *TUB4.* However, strain ESM183 carrying the *ADH-Xgam* construct on a *LEU2*-based plasmid (pSM83) was unable to grow on 5-FOA plates (sector 2). Identical results were obtained by tetrad analysis of strain ESM178 (*TUB4/Δtub4::HIS3*) containing *ADH-Xgam.* Only two of the four spores from each tetrad formed colonies. These were His^-, indicating that they carried the functional *TUB4.* Expression of *Xgam* in yeast was confirmed by Xgam-specific antibodies (Fig. 1 *A*). In summary, we conclude that Xgam does not fulfill Tub4p function.

Tub4p Is Associated with the Inner and Outer Plaques of the SPB

A functional epitope-tagged Tub4p–HA fusion protein was shown to be localized at the SPB by indirect immunofluorescence (Sobel and Snyder, 1995). Since functions for some SPB substructures have been deduced from ultrastructural analysis (Byers and Goetsch, 1975), knowing the localization of Tub4p with SPB substructures will certainly help to understand the role of this protein. Affinity-purified antibodies against a carboxy-terminal portion of

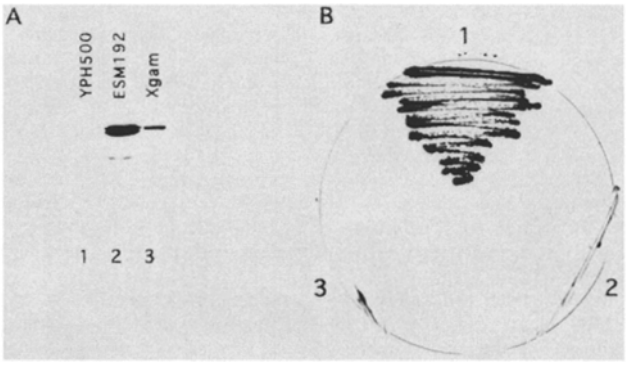

Figure 1. The γ-tubulin from *X. laevis* does not complement for *TUB4.* (*A*) Expression of γ-tubulin from *X. laevis* in *S. cerevisiae.* Yeast extracts (80 μg) of YPH500 (*TUB4*; lane *1*), ESM192 (*ADH-Xgam*; lane *2*), and an extract from *X. laevis* eggs (lane *3*) were analyzed by immunoblotting with peptide antibodies specific to *X. laevis* γ-tubulin. (*B*) *X. laevis* γ-tubulin does not complement for Tub4p. Growth of strain ESM183 (*Δtub4::HIS3* and *TUB4* on the *URA3*-based plasmid pRS316) carrying plasmids pSM204 (*TUB4* on the *LEU2*-based pRS315; sector 1), the *Xgam* expression plasmid pSM83 (*ADH-Xgam* on pRS315; sector 2), or pRS315 (sector 3) on 5-FOA plates at 23°C. Failure of ESM183 pRS315-*ADH-Xgam* to grow on 5-FOA plates (sector 2) indicates that Xgam does not provide Tub4p functions in *S. cerevisiae.*

Tub4p were used for the localization studies. The specificity of these antibodies toward Tub4p was investigated by immunoblotting. Tub4p was not detected in the total yeast extract (Fig. 2 *A*, lane *1*); however, in a fraction enriched for nuclei, a band at ~55 kD reacted with the antibodies (lane *2*). A protein with the same migration behavior was stained in a total yeast extract after expression of *TUB4* from the strong *GAL1* promoter (lane *3*). These results suggest that our anti-Tub4p antibodies are specific towards Tub4p. Remarkably, although expression of *TUB4* from the *GAL1* promoter results in an at least 100-fold increase in Tub4p levels (Fig. 2 *A*), viability, cell morphology, and microtubule structure were not affected even after a 24-h incubation under inducing conditions (data not shown).

To test whether the affinity-purified anti-Tub4p antibodies stain the SPB, the localization of Tub4p in yeast cells was investigated by indirect immunofluorescence microscopy. Tub4p was localized as one or two dots on the nuclear periphery of the cells (Fig. 2 *B*). The number of Tub4p signals per cell and their location are in agreement with an association of Tub4p with the SPB. That the Tub4p signal was associated with the SPB was confirmed by a double labeling experiment using antibodies against the 90-kD SPB protein (Rout and Kilmartin, 1990) as a marker for SPBs (data not shown). Unfortunately, the affinity-purified antibodies lost their activity quite rapidly. To circumvent this problem, a functional gene fusion of *TUB4* with a sequence coding for three repeats of the hemagglutinin (HA) epitope was constructed. Tub4p-HA was expressed in yeast and was associated with the SPB in indirect immunofluorescence experiments (data not shown).

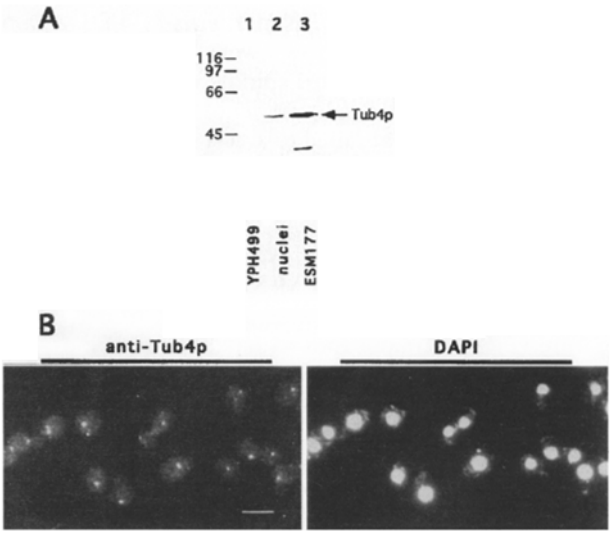

Figure 2. Tub4p is a component of the SPB. (*A*) Specificity of the anti-Tub4p antibodies. Total extract from strain YPH499 (80 μg; lane *1*), enriched nuclei of YPH499 (80 μg; lane *2*), or extract from ESM177 (*GAL1-TUB4*; 40 μg, lane *3*) were separated by SDS-PAGE and analyzed by immunoblotting with affinity-purified anti-Tub4p antibodies. Strain ESM177 had been grown in galactose medium to induce *GAL1-TUB4*. (*B*) Immunofluorescence microscopy of BJ5626 cells (gift of B. Jones, Carnegie-Mellon University, Pittsburgh, PA) stained with affinity-purified anti-Tub4p antibodies. DNA was stained with DAPI. Bar, 2.5 μm.

At least eight substructures of the SPB are detectable by EM (see Fig. 8 *A*). Most importantly, the outer and inner plaques organize the cytoplasmic and nuclear microtubules, respectively (Byers, 1981*a*; Byers and Goetsch, 1975). An SPB component involved in microtubule organization should, therefore, localize to the outer and inner plaques of the SPB. The localization of Tub4p with the SPB was determined by immunoelectron microscopy using enriched SPBs and affinity-purified anti-Tub4p antibodies. The ultrathin sections showed numerous SPBs of which ~200 were inspected more closely. The substructures of the SPB—outer, central, and inner plaques—were clearly detectable (Fig. 3, *A–D*). In addition, the embedded SPBs contained nuclear microtubules attached to the inner plaque, while the cytoplasmic microtubules were lost during the purification of the SPBs (Rout and Kilmartin, 1990). Two to seven gold particles were associated with ~70% of the sectioned SPBs. These gold particles were localized with the inner (up to four gold particles; Fig. 3, *A–C*; note *B* is an enlargement of *A*) and outer (up to three; Fig. 3, *B* and *D*) plaques of the SPB. To confirm this result, thin sections of isolated SPBs from *TUB4-HA* and *TUB4* cells were incubated with 12CA5 antibodies that are directed against the HA epitope. While none of the *TUB4* SPBs were labeled, 30% of the SPBs from *TUB4-HA* cells had two to three gold particles associated with the inner plaque (Fig. 3, *E* and *F*) and to a lower extent with the outer plaque. Labeling of only 30% of the SPBs may be explained by the fixation sensitivity of the HA-antigen (Spang et al., 1995). In the experiments using the anti-Tub4p and anti-HA antibodies, SPB staining was not observed when sections of SPBs were incubated with the secondary antibody, only indicating that the labeling was dependent on the primary antibodies. Taken together, our results suggest that Tub4p is associated with the sites of microtubule attachment, the inner and the outer plaques of the SPB.

Spindle Elongation Is Defective in tub4-1 Cells

To study the function of Tub4p at the SPB, a conditional lethal mutant of *TUB4* was constructed. Sequence analysis of the recessive *tub4-1* allele revealed that the mutated *Tub4p** carried a Phe243Ser substitution. *tub4-1* was integrated in its chromosomal location (ESM208). Some mutants affecting microtubule function in *S. cerevisiae* display supersensitivity to the anti-microtubule drug benomyl (Stearns et al., 1990). Cells of *tub4-1*, however, showed no increased sensitivity towards benomyl (data not shown).

To determine whether the *tub4-1* cells exhibited a uniform arrest phenotype, we shifted an asynchronous culture to the restrictive temperature. More than 80% of the *tub4-1* cells completed S phase (Fig. 4 *A*) and arrested in the cell cycle with a single large bud after 3 h at 37°C (data not shown). The number of cells with 2N DNA content, as well as cells with a large bud, declined to 70% after 6 h at 37°C, suggesting that some cells could overcome cell cycle arrest. The nuclear DNA and microtubule organization was visualized by 4′,6-diamidino-2-phenylindole (DAPI) staining and indirect immunofluorescence, respectively. A *TUB4* strain showed characteristic microtubule structures representing all stages of the cell cycle (Fig. 4 *C*, Table II).

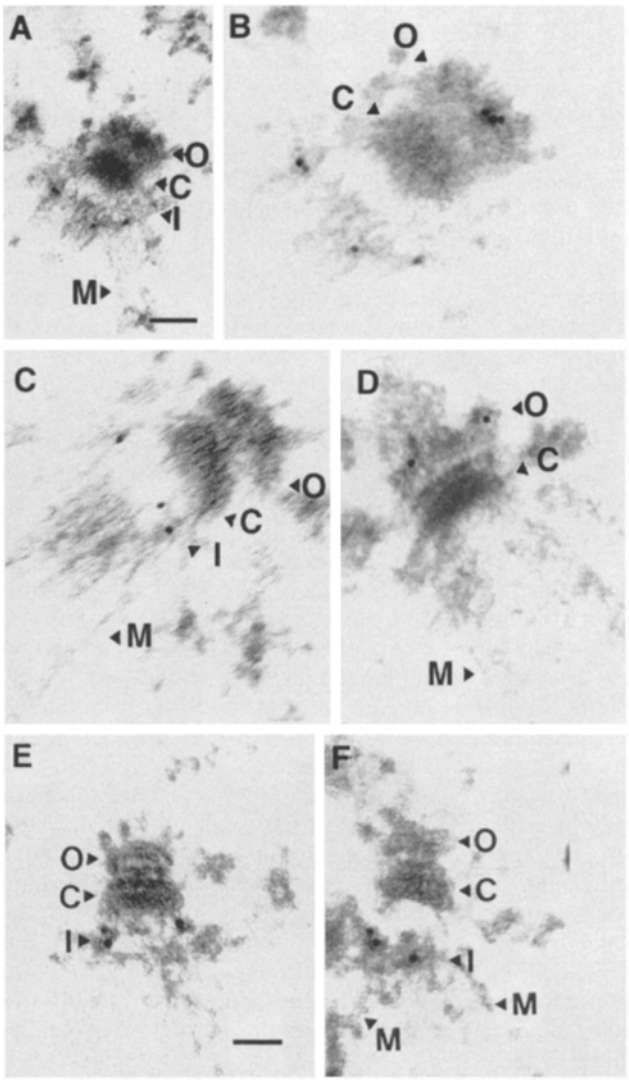

Figure 3. Tub4p is a component of the inner and outer plaques of the SPB. Sections of enriched SPBs of *TUB4* (*A–D*) or *TUB4-HA* cells (*E* and *F*) were incubated with affinity-purified anti-Tub4p (*A–D*) or anti-HA (12CA5) antibodies followed by protein A–gold (*A–D*) or rabbit anti–mouse IgGs followed by protein A–gold (*E* and *F*). (*A–D*) SPBs with Tub4p staining (10 nm gold particles) at the inner and outer plaques. *B* is an enlargement of *A*. Four gold particles are associated with the inner plaque (*A*) and three (*B*) at the outer plaque of the SPB. (*C*) SPB with three gold particles at the inner plaque. (*D*) SPB with two Tub4p signals at the outer plaque. (*E* and *F*) Tub4p-HA staining at the inner plaque (three gold particles). *C*, central plaque; *I*, inner plaque; *M*, microtubules; *O*, outer plaque. Bars: (*A*) 160 nm; (*E*) 80 nm. *B–D* is double the size of *A*; *F* is the same magnification as *E*.

In particular, wild-type large budded cells contained an anaphase spindle with DAPI-staining regions in both the mother and bud cell bodies. While *tub4-1* cells grown at the permissive temperature were similar to wild-type cells (data not shown), *tub4-1* cells incubated at the nonpermissive temperature displayed four classes of abnormal spindles. Large-budded cells with a very short spindle, a metaphase-like bipolar spindle, or a monopolar spindle, and unbudded cells with a short bipolar spindle were observed (Fig. 4 *B*). The distribution of these spindle structures is given in Table II. Interestingly, in >90% of the large budded *tub4-1* cells, the cytoplasmic microtubules responsible for nuclear migration appeared elongated. We investigated whether nuclear migration occurs in *tub4-1* cells. A mutation that interferes only with nuclear but not with cytoplasmic microtubule function causes cells to arrest with an undivided nucleus located in the bud neck. In comparison, 85% of *tub2-401* cells that lack all microtubules have a defect in nuclear migration (Huffaker et al., 1988). In ~50% of *tub4-1* cells, the nucleus was located in the mother cell body, indicating a partial defect in nuclear migration.

The formation of a short spindle in the *tub4-1* mutant suggested that the SPB was duplicated and separated. To determine if this was indeed the case, we stained cells with antibodies against the 90-kD SPB component. In ~90%, two SPBs were detected in cells (n = 200) with a large bud confirming that SPBs were duplicated and separated in most *tub4-1* cells (data not shown).

About 20% of *tub4-1* cells arrested in the cell cycle without a bud. We tested whether these cells were in a specific cell cycle stage at the time the culture was shifted to the nonpermissive temperature. As for an unsynchronized culture, 76% of α-factor–synchronized *tub4-1* cells arrested with a large bud in the first cell cycle (data not shown). Microtubule staining of these cells was very similar to that of an unsynchronized *tub4-1* population. In 90% of *tub4-1* cells (n = 200) with a large bud, two SPBs were detected using the 90-kD SPB antigen as marker (Fig. 4 *D*). Again, 24% of the arrested *tub4-1* cells were unbudded, half of which contained either a short spindle or no nucleus (Table II). These unbudded cells rose most likely from large-budded *tub4-1* cells that failed to arrest in the cell cycle.

tub4-1 Cells Are Defective in Mitotic Spindle Formation

To understand the defect of *tub4-1* cells, the spindle morphology was investigated by EM. SPBs of wild-type (Fig. 5 *A*) and *tub4-1* cells incubated at the nonpermissive temperature (Fig. 5 *B*) appeared to have identical morphology. SPBs were embedded in the nuclear envelope, and nuclear microtubules were in association with the SPB. At the restrictive temperature, however, nuclear microtubules of *tub4-1* cells were severely disorganized. Sections through seven *tub4-1* cells showing two SPBs, of which two are shown in Fig. 5, *C* and *D*, were inspected more closely. No obvious defect in SPB structure was apparent. SPBs were embedded into the nuclear envelope via the central plaque. The half bridge and the outer plaque appeared normal. Since the inner plaque is hardly visible in sections

Figure 4. Cell cycle arrest of *tub4-1* cells. (*A*) *tub4-1* (ESM208) and *TUB4* cells (YPH500) were grown in YPD medium at 23°C. Both cultures were then shifted to 37°C. Samples were taken after 3 and 6 h. The DNA content of 20,000 cells was determined by flow cytometry. (*B*) Tubulin and DAPI staining of *tub4-1* cells. *tub4-1* cells pregrown at 23°C were incubated for 3 h at 37°C. Cells were fixed for 1 h and stained with the anti-tubulin antibody WA3. DNA was stained with DAPI. The arrow in *B* points to a short spindle. (*C*) *TUB4* cells

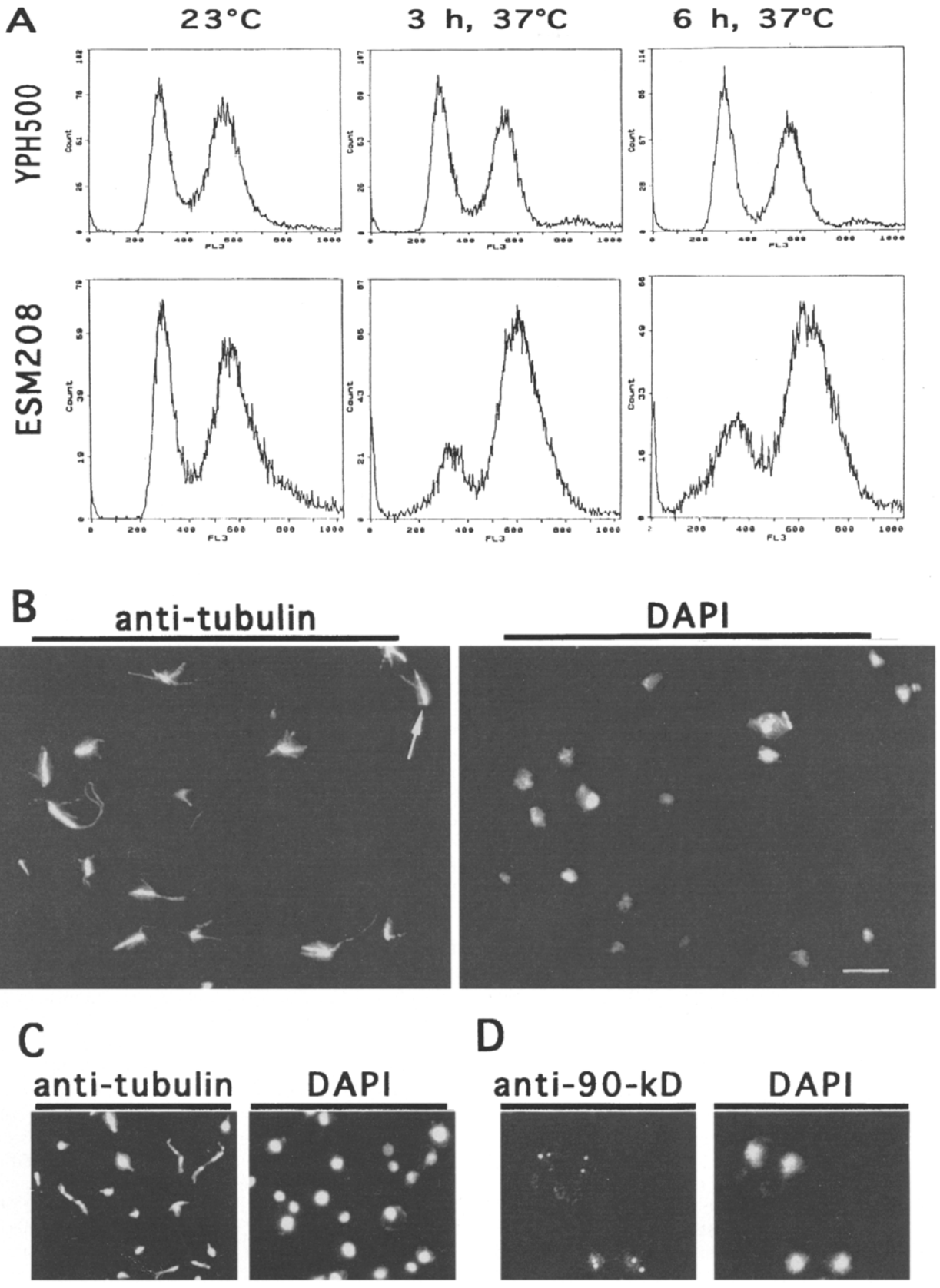

(YPH500) were incubated and prepared for immunofluorescence as described in *B*. (*D*) *tub4-1* cells (strain YAS5; *tub4-1Δsst1::URA3*) were synchronized by α-factor. Cells were released from the cell cycle block and incubated at 37°C for 2 h. Cells were fixed with methanol and acetone, and SPBs were detected by indirect immunofluorescence with anti–90-kD antibodies. DNA was stained with DAPI. Bar, 5.0 μm. *C* and *D* are the same magnification as *B*.

Table II. Spindle Structure and Nucleus Position of tub4-1 Cells

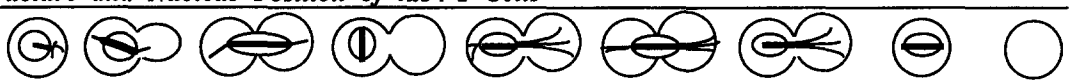

TUB4	42 %	37 %	21 %	0 %	0 %	0 %	0 %	0 %	0 %
tub4-1:									
YAS5 (synchronized)	11 %	0 %	0 %	3 %	44 %	18 %	11 %	6 %	7 %
ESM208 (unsynchronized)	10 %	0 %	0 %	5 %	40 %	24 %	11 %	5 %	5 %

Logarithmic cultures of YPH500 (*TUB4*) and ESM208 (*tub4-1*) were shifted for 3 h to 37°C and prepared for immunofluorescence microscopy. Cells of YAS5 (*tub4-1Δsst1*) were synchronized upon addition of α-factor at 23°C. Synchronized cells were then washed with prewarmed (37°C) YPD medium in order to release the cells from the cell-cycle block. After 2 h at 37°C samples were taken and prepared for immunofluorescence microscopy using anti-tubulin antibodies. DNA was stained with DAPI. The position of the nucleus and the morphology of the spindle of 300 cells were determined. The average of two independent experiments is indicated.

through whole cells, it is difficult to judge whether this SPB substructure is defective in *tub4-1* cells. SPBs were separated, however, located on one side of the nucleus and not connected by a parallel array of microtubules. Instead, the few microtubules spread out and passed the other SPB (Fig. 5 *C*). The distance between the two SPBs was variable. SPBs were close together (Fig. 5 *D*) or separated by 0.5–1 μm. The electronmicrographs are in agreement with the spindle phenotypes of *tub4-1* cells (Fig. 4 *B*) observed by indirect immunofluorescence. The defective spindle in Fig. 5 *C* corresponds with the short microtubule bundles seen in large-budded *tub4-1* cells. The two SPBs close to each other (Fig. 5 *D*) are consistent with the monopolar spindle seen in some *tub4-1* cells. Two classes of microtubule defects were observed when sections through SPBs (n = 20) were inspected. Attached nuclear microtubules were either severely disorganized, pointing in another direction than the axis of the SPB (n = 15; Fig. 5, *E* and *F*), or SPBs of *tub4-1* cells had no or only a few detectable microtubules (n = 5; Fig. 5, *G* and *H*).

Since microtubules are required for SPB separation (Jacobs et al., 1988), the defect in spindle formation in *tub4-1* cells may be explained by nonfunctional nuclear microtubules. Alternatively, a spindle may form that then collapses at a later stage in the cell cycle. Such a spindle collapse was observed after eliminating the function of the kinesin-related proteins Kip1p and Cin8p. In the *kip1cin8* double mutant, preanaphase bipolar spindles rapidly collapsed, with previously separated poles being drawn together (Saunders and Hoyt, 1992).

These possibilities were tested using HU-blocked *tub4-1* cells. HU prevents DNA replication and arrests cells with a short spindle at the end of S or in G2 phase of the cell cycle (Hartwell, 1976). If the defect in microtubule organization of *tub4-1* cells occurred after spindle formation, the HU-blocked cells should have a normal spindle. *tub4-1* cells were synchronized in G1 of the cell cycle by the addition of α-factor. Cells were then released from cell cycle arrest at 37°C with or without HU. As controls, wild-type and *cdc15* cells were also synchronized by α-factor, and then shifted to 37°C. *cdc15* cells arrest in the cell cycle with elongated spindles at the end of mitosis (Schweitzer and Philippsen, 1991). Analysis of DNA content by flow cytometry confirmed that DNA replication was inhibited by HU (data not shown). Microtubule organization was analyzed by EM. No obvious defect in spindle formation was observed in HU-blocked *tub4-1* cells (n = 5; Fig. 6 *A*). The two separated SPBs were connected by an ordered, parallel array of microtubules. We noticed that in some cases (n = 3), the spindle was located more toward one side of the nucleus. However, such spindles were also observed in *tub4-1* cells incubated at the permissive temperature (data not shown). In contrast, *tub4-1* cells not incubated with HU replicated the DNA and revealed defective spindles. In sectioned cells where two SPBs (n = 3) were observed, no ordered array of microtubules characteristic of a short spindle was detectable (Fig. 6 *B*). As for an unsynchronized culture, the two SPBs were located on the same side of the nucleus. The spindle in wild-type or *cdc15* cells was of normal appearance (data not shown). Single SPBs of *TUB4*, *cdc15*, and *tub4-1* cells were inspected more closely. All SPBs from *cdc15* and *TUB4* cells and most of the SPBs from *tub4-1* cells blocked by HU were associated with a parallel array of nuclear microtubules (Table III). In contrast, SPBs of *tub4-1* cells had in a single section only few or misdirected microtubules similar to the phenotypes observed for an unsynchronized *tub4-1* culture (Fig. 5, *E–H*). In summary, our results are consistent with the formation of a short spindle in *tub4-1* cells that then collapses at later stages in the cell cycle.

Chromosome Loss Is Increased in tub4-1 Cells

An expected phenotypic consequence of mitotic spindle malfunction is a decrease in the fidelity of chromosome transmission (Hoyt et al., 1990). This was investigated using the indicator strain YRN212 carrying *SUP11* on a supernumerary chromosome. *SUP11* suppresses the *ade2-101* phenotype of YRN212. Therefore, loss of the *SUP11*-containing chromosome causes a phenotypic change in colony color from white to red. *tub4-1* was integrated into strain YRN212, creating a duplication containing the wild-type copy and the mutant copy flanking plasmid sequences (YAS3). Cells of YAS3 that spontaneously excised *TUB4* were selected for on 5-FOA plates (YAS4). Chromosome loss of strains YRN212, YAS3, and YAS4 was determined at different temperatures (Table IV). Even at the permissive temperature, chromosome loss of *tub4-1* cells was increased at least twofold compared to *TUB4* cells. At 30° and 33°C, 50% and 74% of *tub4-1* cells had defects in chromosome transmission, while the control strains were not affected (Table IV).

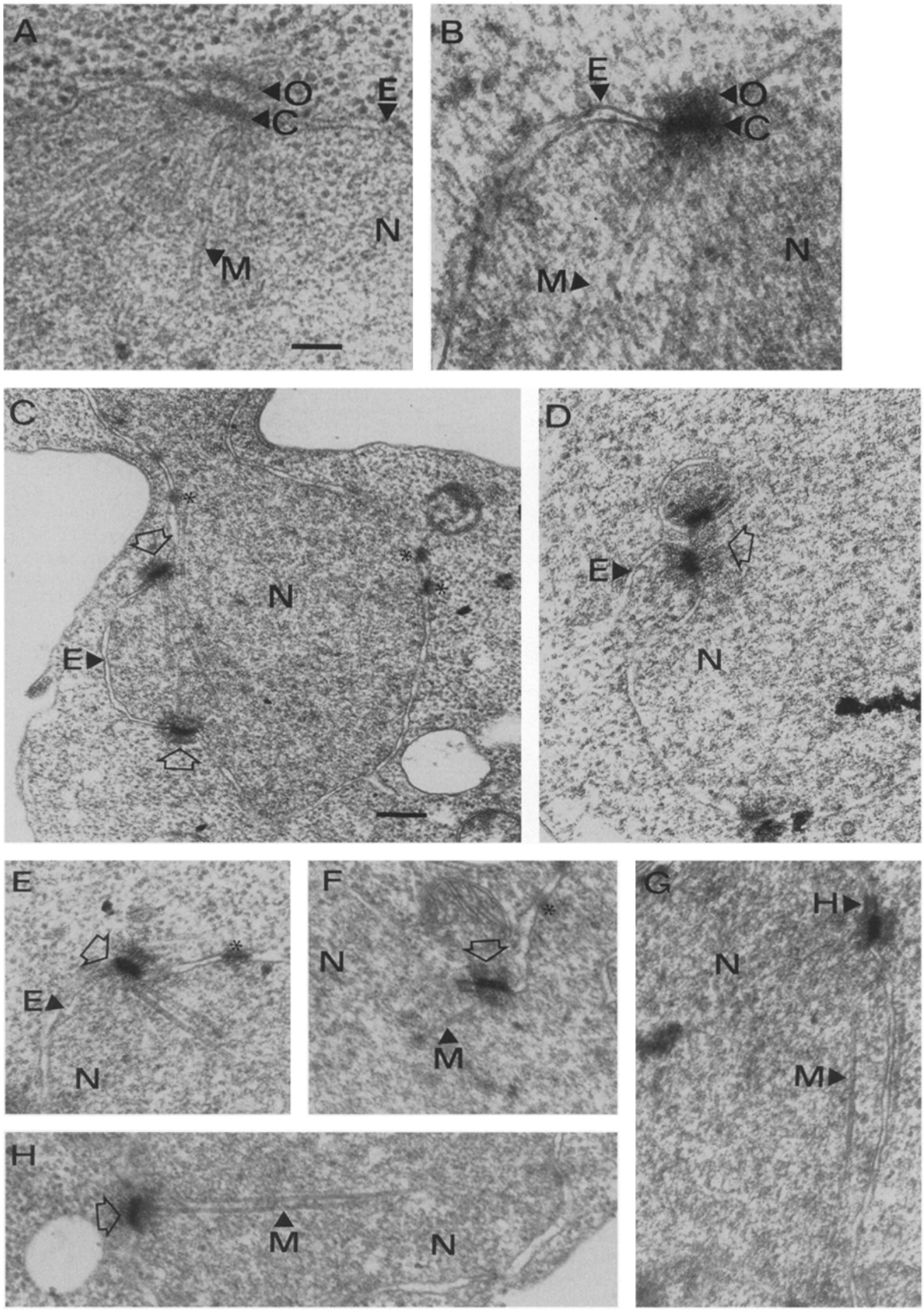

Figure 5. Spindle and SPB morphology of *tub4-1* cells. *TUB4* (*A*) and *tub4-1* cells (*B–H*) were grown at 23°C. Cells were either incubated at 23°C (*B*) or shifted to 37°C for 3 h (*C–H*). Sections of cells with two SPBs (*C* and *D*) or one SPB (*A*, *B*, and *E–H*) are shown. Asterisks indicate the position of some nuclear pores. The large arrows in *C–F* and *H* point towards SPBs. *C*, central plaque; *E*, nuclear envelope; *H*, half bridge; *N*, nucleus; *O*, outer plaque; *M*, microtubules. Bars: (*A*) 100 nm; (*C*) 200 nm. *B* is the same magnification as *A*. *D–H* are the same magnification as *C*.

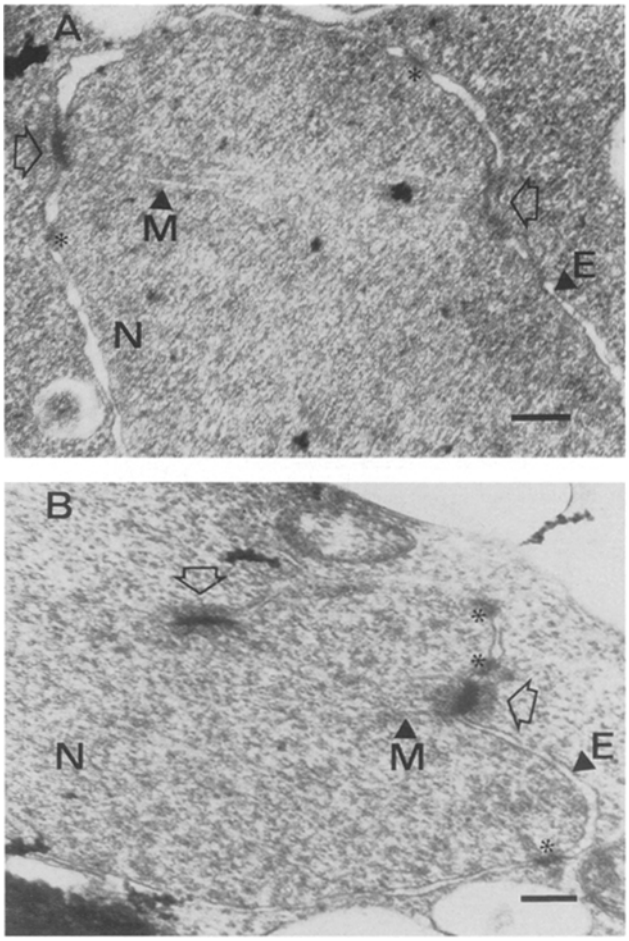

Figure 6. tub4-1 cells form a short spindle. *tub4-1* cells (YAS5; *tub4-1Δsst1::URA3*) were synchronized with α-factor. Cells were released in YPD medium with (*A*) or without (*B*) HU at 37°C. Cells were incubated for 2 h at 37°C, and then prepared for EM. (*A*) Shown is a *tub4-1* cell arrested in the cell cycle with HU. The two SPBs are connected by a short spindle. (*B*) Synchronized *tub4-1* cells without HU treatment. The separated SPBs were not connected by a parallel array of microtubules. Asterisks indicate the position of some nuclear pores. The large arrows point toward SPBs. *E*, nuclear envelope; *N*, nucleus; *M*, microtubules. Bars: (*A*) 200 nm; (*B*) 150 nm.

Cell Cycle Arrest and Survival of tub4-1 Cells Is Dependent on the Checkpoint Control Gene BUB2

A defect in microtubule function activates mitotic checkpoint control, causing *BUB* and *MAD* gene-dependent cell cycle arrest (Hoyt et al., 1991; Li and Murray, 1991). We tested whether the cell cycle arrest of *tub4-1* cells is dependent on mitotic checkpoint control. The checkpoint control gene *BUB2* (Hoyt et al., 1991) of ESM208 (*tub4-1*) was disrupted (ESM215; *tub4-1bub2*). While both strains formed colonies at 30°C, only *tub4-1* cells grew at 33°C (data not shown). Furthermore, inactivation of *BUB2* decreased the viability of *tub4-1* cells shifted to 37°C (Fig. 7 *A*). More than 60% of the *tub4-1* cells survived an incubation period of 4.5 h at 37°C, indicating that cell cycle arrest of *tub4-1* cells is in part reversible. In contrast, only 10% of *tub4-1bub2* cells were viable after 4.5 h at 37°C (Fig. 7 *A*).

Table III. Nuclear Microtubules of tub4-1 Cells Are not Properly Attached to the SPB

YAS7 (*TUB4*) (n= 22)	99 %	0 %	1 %
YAS9 (*cdc15*) (n= 21)	100 %	0 %	0 %
YAS5 (*tub4-1*) (n= 31)	10 %	22 %	68 %
YAS5 (*tub4-1*) HU (n= 24)	92 %	0 %	8 %

Early log-phase cells of each strain were arrested with α-factor for 2 h at 23°C and then shifted to 37°C for 1 h. Cells were released in 37°C prewarmed YPD medium. In the experiment YAS5 HU, 0.1 M HU was present in the medium after cell-cycle release. About 80% of the cells proceed further in the cell cycle as judged by immunofluorescence of cells with anti-tubulin antibodies. After the release for 2 h at 37°C, cells were collected and prepared for electron microscopy. Ultrathin sections of yeast cells were investigated for SPB and spindle morphology.

While *tub4-1* cells arrested in the cell cycle with a single large bud, the *tub4-1bub2* double mutant continued budding (Fig. 7 *B*). Cells with two buds accumulated in the *tub4-1bub2* culture. Taken together, these results clearly demonstrate a role of *BUB2* in the cell cycle arrest of *tub4-1* cells.

Discussion

TUB4 of *S. cerevisiae* encodes a novel tubulin that most resembles the γ-tubulin family. However, Tub4p is with 41% identity only moderately homologous to human γ-tubulin, while the γ-tubulins from *X. laevis*, *D. melanogaster*, *S. pombe*, and *A. nidulans* are 98, 78, 71, and 68% identical to human γ-tubulin, respectively. Tub4p is even less similar to α- (31% identity to Tub1p and Tub3p) and β-tubulin (27%, Tub2p) of *S. cerevisiae*. Based on the analysis of the Tub4p sequence, it has been suggested that Tub4p represents the first member of a new tubulin superfamily (Burns, 1995).

To understand the function of Tub4p in *S. cerevisiae*, we studied the localization of Tub4p with substructures of the SPB. In addition, the phenotype of the conditional lethal *tub4-1* allele was analyzed. *tub4-1* cells arrested in the first cell cycle after shifting the cells to the nonpermissive temperature, assuring that the observed defects are a direct consequence of Tub4p malfunction. Our analysis suggests

Table IV. Temperature-dependent Chromosome Loss of tub4-1 Cells

Strain	23°C	30°C	33°C
	%	%	%
YRN212	1.2 ± 0.2	0.75 ± 0.35	0.5
YAS3	2.0 ± 1.4	2.9 ± 1.4	2.2
YAS4	4.4 ± 1.8	50.1 ± 10.4	74

For the determination of chromosome loss, 200 cells were plated on YPD plates and incubated for 5 d at the indicated temperatures. Red and sectored colonies indicated chromosome loss. YRN212 (*TUB4*) represents 2, YAS3 (*tub4-1/TUB4*) represents 3, and YAS4 (*tub4-1*) represents 10 individual experiments. The values obtained at 33°C represent a single experiment.

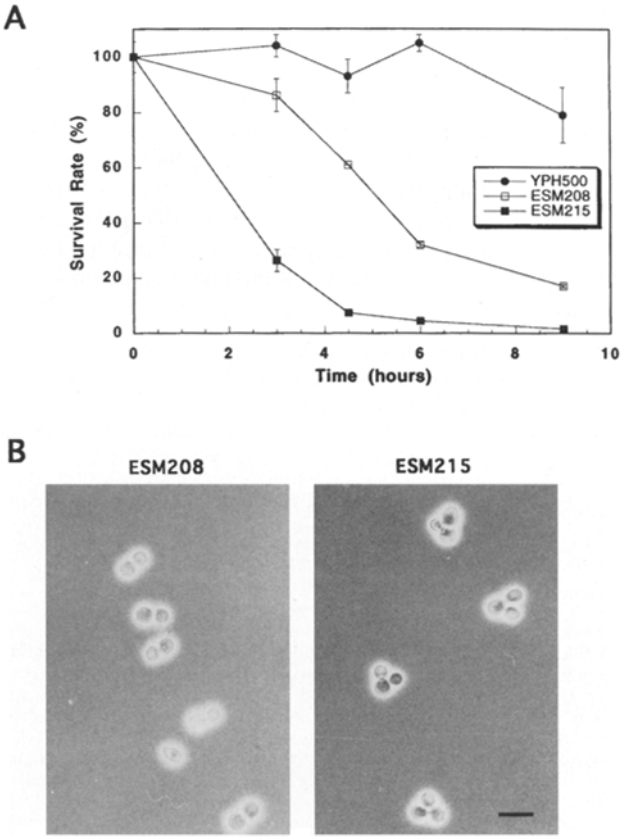

Figure 7. Cell cycle arrest of *tub4-1* cells is dependent on the mitotic checkpoint control gene *BUB2*. (*A*) Survival rate. *TUB4* (YPH500), *tub4-1* (ESM208), and *tub4-1bub2* cells (ESM215) were incubated at 37°C for the indicated times. Equal numbers of cells were plated onto YPD plates at 23°C. The average of three independent experiments is shown. (*B*) Morphology of *tub4-1* and *tub4-1bub2* cells. *tub4-1* and *tub4-1bub2* were incubated for 4 h at 37°C. Bar, 5.0 μm.

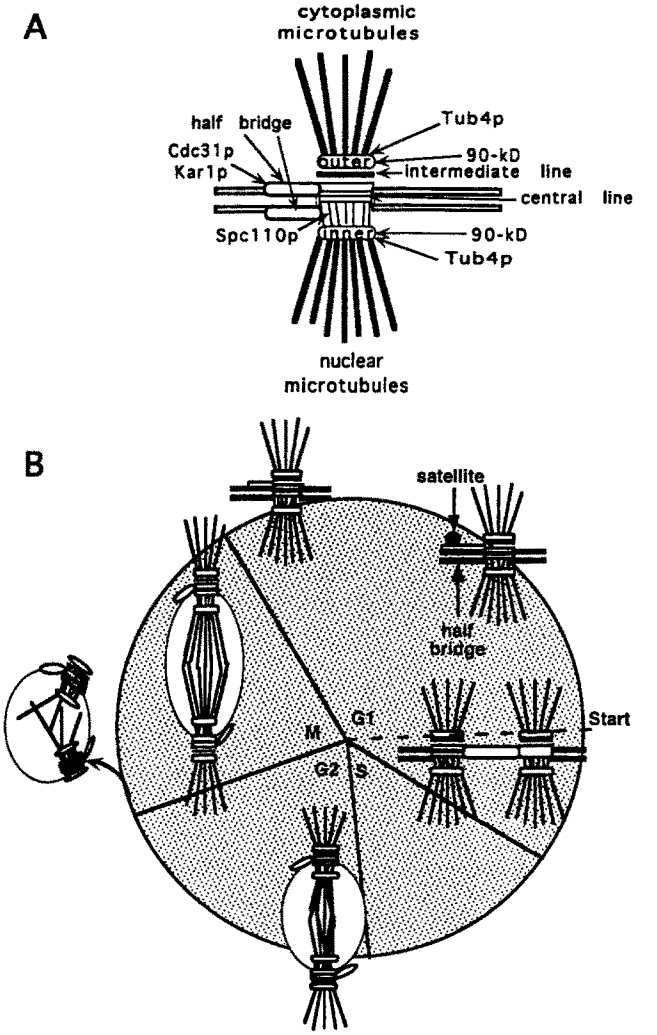

Figure 8. Localization of SPB proteins: model for the defect of *tub4-1* cells. (*A*) Schematic diagram showing the localization of Tub4p relative to that of the known SPB components Cdc31p (Spang et al., 1993), Karlp (Spang et al., 1995), Spc110p (Rout and Kilmartin, 1990), and 90-kD protein (Rout and Kilmartin, 1990). (*B*) Model for the defect of *tub4-1* cells.

that *TUB4* has important functions in microtubule organization. First, the essential Tub4p is associated with the SPB (Fig. 2 *B*). Closer inspection showed that Tub4p is a component of the inner and the outer plaques of the SPB (Fig. 3)—exactly the sites of the SPB that organize the nuclear and cytoplasmic microtubules, respectively (Fig. 8 *A*, Byers and Goetsch, 1975). Second, 50% of *tub4-1* cells are defective in nuclear migration (Table II), which is most likely caused by nonfunctional astral microtubules (Sullivan and Huffaker, 1992). Third, *tub4-1* cells fail to form a mitotic spindle (Figs. 4–6). Fourth, cell cycle arrest and survival of *tub4-1* cells is dependent on the mitotic checkpoint control gene *BUB2* (Fig. 7). Since *BUB2* is required for proper cell cycle arrest in mitosis in response to the loss of microtubule function (Hoyt et al., 1991), *BUB2*-dependent cell cycle arrest and survival of *tub4-1* cells suggests a defect in microtubule organization. Finally, *tub4-1* cells lose a supernumerary chromosome at elevated rates during mitotic growth (Table IV). Some mutants with decreased fidelity in chromosome transmission are defective in microtubule structure (Hoyt et al., 1990, 1992). Examples are mutations in the two genes coding for α-tubulin in *S. cerevisiae*, and in *CIN8* and *KIP1* that encode polypeptides related to the heavy chain of the motor protein kinesin (Hoyt et al., 1992).

While our manuscript was in preparation, Sobel and Snyder (1995) published a study on Tub4p function based on the partial depletion of Tub4p. They reported multiple defects in spindle formation and a defect in nuclear migration. These deficiencies were observed 17–20 h (or 8.1±0.6 generations) after repression of *GAL1-TUB4* by glucose. Since Tub4p levels were not controlled in these experiments, it is unclear whether the described phenotypes are a direct or indirect consequence of Tub4p depletion. Using a similar *GAL1-TUB4* depletion strain, we found by indirect immunofluorescence drastically different Tub4p levels in individual cells after growth for 24 h in the repressing glucose medium (E. Schiebel, unpublished results). This may explain the multiple phenotypes of *GAL1-TUB4* cells seen after repression of the *GAL1* promoter.

What is the role of Tub4p in microtubule organization?

The localization of Tub4p with the SPB substructures that are in contact with microtubule ends (Fig. 3) suggests that Tub4p may be involved in microtubule nucleation and/or attachment of microtubules to the SPB. A model for Tub4p's functions has to consider the phenotype of *tub4-1* cells. *tub4-1* cells incubated at the nonpermissive temperature duplicate and separate their SPBs. Furthermore, formation of a short bipolar spindle appears normal as suggested by the HU experiment (Fig. 6; Table III). Since mitotic spindles were not observed in *tub4-1* cells, it is most likely that the defects in microtubule organization occur after the formation of a short bipolar spindle (Fig. 8 *B*). It is important to emphasize that only a subset of Tub4p's functions may be affected in *tub4-1* cells. Therefore, we cannot exclude that *tub4* alleles defective in other *TUB4* functions may reveal different phenotypes.

A number of yeast mutants with defects in mitotic spindle formation have been described. For example, in cells carrying the cold-sensitive *tub2-405* allele, the short bipolar spindle collapsed at the nonpermissive temperature with both SPBs on opposite poles of the nucleus (Pasqualone and Huffaker, 1994). A similar phenotype was observed when cells containing short spindles were treated with nocodazole. The spindles collapsed, but the SPBs remained on opposite sides of the nucleus (Jacobs et al., 1988). In contrast, inactivation of the kinesin-related motor proteins Cin8p and Kip1p caused rapid collapse of preanaphase spindles, with previously separated SPBs being drawn together (Saunders and Hoyt, 1992). This phenotype was explained by counteracting forces produced by kinesin-related proteins. Since the SPBs were on the same side of the nucleus also in *tub4-1* cells, it is likely that the defective microtubule structure disturbs the counteracting forces, such that the separated SPBs are drawn together. Assuming that the attachment of nuclear microtubules to the SPB is weakened in *tub4-1* cells, the detachment of some microtubules could be caused by mitosis-specific pulling forces that are transmitted to the SPB via microtubules. Mitosis-specific forces that may act on the MTOC are indicated by chromosome and spindle movements, including chromosome congression to the metaphase plate and sister chromatid separation in anaphase A (for review see McIntosh and Koonce, 1989). Microtubule detachment is consistent with the observation that some *tub4-1* SPBs are in contact with only a few microtubules (Fig. 5; Table III). Detachment of nuclear microtubules from the SPB may then disturb the counteracting forces, resulting in spindle collapse.

Although the immunoelectron microscopic analysis revealed a close proximity of Tub4p and microtubules at the SPB (Fig. 3), it is not clear whether Tub4p directly interacts with microtubule ends. Tub4p could function either as a structural component of the inner and outer plaques of the SPB or as the direct link between microtubule ends and the SPB. Interestingly, microtubule ends proximal to the site of initiation on the SPB are sealed because of a terminal component connecting the walls of the microtubule cylinder (Byers et al., 1978). It is tempting to speculate that Tub4p is part of this microtubule cap structure. Interestingly, a microtubule cap with a somewhat different structure formed by a γ-tubulin–containing complex at the minus ends of microtubules was identified by in vitro (Zheng et al., 1995) and in situ (Moritz et al., 1995) studies. The identification of proteins interacting with Tub4p will further elucidate Tub4p's role in microtubule organization. We recently identified suppressors of *tub4-1*, one of which encodes the 90-kD SPB component that is associated with the same SPB substructures as Tub4p (Fig. 8 *A*). In addition, we obtained evidence that Tub4p interacts with the 90-kD SPB component (Geissler et al., 1996). Taken together, Tub4p may be a highly divergent γ-tubulin adapted to the specialized microtubule attachment structures in *S. cerevisiae*.

M. Matzner is acknowledged for technical support and Dr. T. Schuster (University of Würzburg, Germany) for helpful discussions. We thank Dr. J. Kilmartin for carefully reading our manuscript.

This work was supported by a grant from the Bundesministerium für Forschung und Technologie.

Received for publication 23 January 1996 and in revised form 5 April 1996.

References

Ausubel, F.M., R. Brent, R.E. Kingston, D.D. Moore, J.G. Seidman, J.A. Smith, and K. Struhl. 1994. Current protocols in molecular biology. *In* Current Protocols. John Wiley & Sons, Inc., New York.

Baum, P., C. Furlong, and B. Byers. 1986. Yeast gene required for spindle pole body duplication: homology of its product with Ca^{2+}-binding proteins. *Proc. Natl Acad. Sci. USA.* 83:5512–5516.

Bradford, M.M. 1976. A rapid and sensitive method for the quantitation of microgram quantities of protein utilizing the principle of protein-dye binding. *Anal. Biochem.* 72:248–254.

Burns, R.G. 1995. Analysis of the γ-tubulin sequences: implications for the functional properties of γ-tubulin. *J. Cell Sci.* 108:2123–2130.

Byers, B. 1981*a*. Multiple roles of the spindle pole bodies in the life cycle of *Saccharomyces cerevisiae*. *In* Molecular Genetics in Yeast. Vol. 16. D. Wettstein, A. Stenderup, M. Kielland-Brandt, and J. Friis, editors. Alfred Benzon Symp. Munksgaard, Copenhagen. 119–133.

Byers, B. 1981*b*. Cytology of the yeast life cycle. *In* The Molecular Biology of the Yeast *Saccharomyces*—Life Cycle and Inheritance. J.N. Strathern, E.W. Jones, and J.R. Broach, editors. Cold Spring Harbor Laboratory, Cold Spring Harbor, NY. 59–96.

Byers, B., and L. Goetsch. 1975. Behavior of spindles and spindle plaques in the cell cycle and conjugation of *Saccharomyces cerevisiae*. *J. Bacteriol.* 124:511–523.

Byers, B., and L. Goetsch. 1991. Preparation of yeast cells for thin-section electron microscopy. *In* Guide to Yeast Genetics and Molecular Biology. C. Guthrie and G.R. Fink, editors. Methods in Enzymology. Vol. 194. Academic Press, New York. 602–607.

Byers, B., K. Shriver, and L. Goetsch. 1978. The role of spindle pole bodies and modified microtubule ends in the initiation of microtubule assembly in *Saccharomyces cerevisiae*. *J. Cell Sci.* 30:331–352.

Cadwell, R.C., and G.F. Joyce. 1992. Randomization of genes by PCR mutagenesis. Cold Spring Harbor Laboratory, Cold Spring, NY. 28–32.

Errabolu, R., M.A. Sanders, and J.L. Salisbury. 1994. Cloning of a cDNA encoding human centrin, an EF-hand protein of centrosomes and mitotic spindle poles. *J. Cell Sci.* 107:9–16.

Geissler, S., G. Peirera, A. Spang, M. Knop, S. Souès, J. Kilmartin, and E. Schiebel. 1996. The spindle pole body component Spc98p interacts with the γ-tubulin-like Tub4p of *S. cerevisiae* at the sites of microtubule attachment. *EMBO (Eur. Mol. Biol. Organ.) J.* In press.

Guthrie, C., and G.R. Fink. 1991. Guide to yeast genetics and molecular biology. *In* Methods in Enzymology. Vol. 194. Academic Press, New York. 12–15.

Harlow, E., and D. Lane. 1988. Antibodies. *In* Antibodies: A Laboratory Manual. Cold Spring Harbor Laboratory, Cold Spring Harbor, NY. 726 pp.

Hartwell, L.H. 1976. Sequential function of gene products relative to DNA synthesis in the yeast cell cycle. *J. Mol. Biol.* 104:803–817.

Horio, T., S. Uzawa, M.K. Jung, B.R. Oakley, K. Tanaka, and M. Yanagida. 1991. The fission yeast γ-tubulin is essential for mitosis and is localized at microtubule organizing centers. *J. Cell Sci.* 99:693–700.

Hoyt, M.A., T. Stearns, and D. Botstein. 1990. Chromosome instability mutants of *Saccharomyces cerevisiae* that are defective in microtubule-mediated processes. *Mol. Cell. Biol.* 10:223–234.

Hoyt, M.A., L. Totis, and B.T. Roberts. 1991. *S. cerevisiae* genes required for cell-cycle arrest in response to loss of microtubule function. *Cell.* 66:507–517.

Hoyt, M.A., L. He, K.K. Loo, and W.S. Saunders. 1992. Two *Saccharomyces cerevisiae* kinesin-related gene products required for mitotic spindle assembly. *J. Cell Biol.* 118:109–120.

Huffaker, T.C., J.H. Thomas, and D. Botstein. 1988. Diverse effects of β-tubu-

lin mutations on microtubule formation and function. *J. Cell Biol.* 106:1997–2010.

Hutter, K.J., and H.E. Eipel. 1979. Microbial determination by flow cytometry. *J. Gen. Microbiol.* 113:369–375.

Jacobs, C.W., A.E.M. Adams, P.J. Szaniszlo, and J.R. Pringle. 1988. Functions of microtubules in the *Saccharomyces cerevisiae* cell cycle. *J. Cell Biol.* 107: 1409–1426.

Joshi, H.C., M.J. Palacios, L. McNamara, and D.W. Cleveland. 1992. γ-tubulin is a centrosomal protein required for cell cycle-dependent microtubule nucleation. *Nature (Lond.).* 356:80–83.

Laemmli, U.K. 1970. Cleavage of structural proteins during the assembly of the head of bacteriophage T4. *Nature (Lond.).* 227:680–685.

Lee, V.D., and B. Huang. 1993. Molecular cloning and centrosomal localization of human caltractin. *Proc. Natl. Acad. Sci. USA.* 90:11039–11043.

Li, Q., and H.C. Joshi. 1995. γ-tubulin is a minus end-specific microtubule binding protein. *J. Cell Biol.* 131:207–214.

Li, R., and A.W. Murray. 1991. Feedback control of mitosis in budding yeast. *Cell.* 66:519–531.

McIntosh, J.R., and U. Euteneuer. 1984. Tubulin hooks as probes for microtubule polarity: an analysis of the method and an evaluation of data on microtubule polarity in the mitotic spindle. *J. Cell Biol.* 98:525–533.

McIntosh, J.R., and M.P. Koonce. 1989. Mitosis. *Science (Wash. DC).* 246:622–628.

Moritz, M., M.B. Braunfeld, J.W. Sedat, B. Alberts, and D.A. Agard. 1995. Microtubule nucleation by γ-tubulin-containing rings in the centrosome. *Nature (Lond.).* 378:638–640.

Oakley, B.R., E. Oakley, Y. Yoon, and M.K. Jung. 1990. γ-tubulin is a component of the spindle pole body that is essential for microtubule function in *Aspergillus nidulans. Cell.* 61:1289–1301.

Pasqualone, D., and T.C. Huffaker. 1994. *STU1*, a suppressor of a β-tubulin mutation, encodes a novel and essential component of the yeast mitotic spindle. *J. Cell Biol.* 127:1973–1984.

Reneke, J.E., K.J. Blumer, W.E. Courchesne, and J. Thorner. 1988. The carboxy-terminal segment of the yeast α-factor receptor is a regulatory domain. *Cell.* 55:221–234.

Rothstein, R.J. 1983. One-step gene disruption in yeast. *Methods Enzymol.* 101: 202–211.

Rout, M.P., and J.V. Kilmartin. 1990. Components of the yeast spindle and spindle pole body. *J. Cell Biol.* 111:1913–1927.

Salisbury, J.L., A. Baron, B. Surek, and M. Melkonian. 1984. Striated flagellar roots: isolation and partial characterization of a calcium-modulated contractile organelle. *J. Cell Biol.* 99:962–970.

Sambrook, J., E.F. Fritsch, and T. Maniatis. 1989. *In* Molecular Cloning: A Laboratory Manual. Cold Spring Harbor Laboratory, Cold Spring Harbor, NY. 545 pp.

Sanger, F., S. Nicklen, and A.R. Coulson. 1977. DNA sequencing with chain-terminating inhibitors. *Proc. Natl. Acad. Sci. USA.* 74:5463–5467.

Saunders, W.S., and M.A. Hoyt. 1992. Kinesin-related proteins required for structural integrity of the mitotic spindle. *Cell.* 70:451–458.

Schiestl, R.H., and R.D. Gietz. 1989. High efficiency transformation of intact yeast cells using stranded nucleic acids as a carrier. *Curr. Genet.* 16:339-346.

Schweitzer, B.I., and P. Philippsen. 1991. *CDC15*, an essential cell cycle gene in *Saccharomyces cerevisiae*, encodes a protein kinase domain. *Yeast.* 7:265–273.

Sikorski, R.S., and P. Hieter. 1989. A system of shuttle vectors and yeast host strains designed for efficient manipulation of DNA in *Saccharomyces cerevisiae. Genetics.* 122:19–27.

Sobel, S.G., and M. Snyder. 1995. A highly divergent γ-tubulin gene is essential for cell growth and proper microtubule organization in *Saccharomyces cerevisiae. J. Cell Biol.* 131:1775–1788.

Spang, A., I. Courtney, U. Fackler, M. Matzner, and E. Schiebel. 1993. The calcium-binding protein cell division cycle 31 of *Saccharomyces cerevisiae* is a component of the half bridge of the spindle pole body. *J. Cell Biol.* 123:405–416.

Spang, A., I. Courtney, K. Grein, M. Matzner, and E. Schiebel. 1995. The Cdc31p-binding protein Kar1p is a component of the half-bridge of the yeast spindle pole body. *J. Cell Biol.* 128:863–877.

Stearns, T., and M. Kirschner. 1994. *In vitro* reconstitution of centrosome assembly and function: the central role of γ-tubulin. *Cell.* 76:623–637.

Stearns, T., L. Evans, and M. Kirschner. 1991. γ-tubulin is a highly conserved component of the centrosome. *Cell.* 65:825–836.

Stearns, T., A.M. Hoyt, and D. Botstein. 1990. Yeast mutants sensitive to antimicrotubule drugs define three genes that affect microtubule function. *Genetics.* 124:251–262.

Sullivan, D.S., and T.C. Huffaker. 1992. Astral microtubules are not required for anaphase B in *Saccharomyces cerevisiae. J. Cell Biol.* 119:379–388.

Sunkel, C.E., R. Gomes, P. Sampaio, J. Perdigao, and C. Gonzáles. 1995. γ-tubulin is required for the structure and function of the microtubule organizing centre in *Drosophila* neuroblasts. *EMBO (Eur. Mol. Biol. Organ.) J.* 14:28–36.

Zheng, Y., K. Jung, and B.R. Oakley. 1991. γ-tubulin is present in *Drosophila melanogaster* and *Homo sapiens* and is associated with the centrosome. *Cell.* 65:817–823.

Zheng, Y., M.L. Wong, B. Alberts, and T. Mitchison. 1995. Nucleation of microtubule assembly by a γ-tubulin-containing ring complex. *Nature (Lond.).* 378:578–583.